NAVAL POSTGRADUATE SCHOOL
MONTEREY, CALIFORNIA

THESIS

THE EFFECTS OF PARTICULATES ON SUPERSONIC SHEAR LAYERS AND AFTERBURNING IN FUEL-RICH PLUMES

by

Siwon R. Lee

December 1995

Thesis Advisor: David W. Netzer

Approved for public release; distribution is unlimited

REPORT DOCUMENTATION PAGE

Form Approved
OMB No. 0704-0188

1. AGENCY USE ONLY (Leave blank)	2. REPORT DATE	3. REPORT TYPE AND DATES COVERED
	December 1995	Master's Thesis

4. TITLE AND SUBTITLE

THE EFFECTS OF PARTICULATES ON SUPERSONIC SHEAR LAYERS AND AFTERBURNING IN FUEL-RICH PLUMES

5. FUNDING NUMBERS

N0001495
95 WR 20016

6. AUTHOR(S)

Lee, Siwon Ray

7. PERFORMING ORGANIZATION NAME(S) AND ADDRESS(ES)

Naval Postgraduate School
Monterey, CA 93943-5000

8. PERFORMING ORGANIZATION REPORT NUMBER

9. SPONSORING/MONITORING AGENCY NAME(S) AND ADDRESS(ES)

Office of Naval Research
800 N. Quincy St.
Arlington, VA 22217-5660

10. SPONSORING/MONITORING AGENCY REPORT NUMBER

11. SUPPLEMENTARY NOTES

The views expressed in this thesis are those of the author and do not reflect the official policy or position of the Department of Defense or the U.S. Government

12a. DISTRIBUTION/AVAILABILITY STATEMENT

Approved for public release; distribution is unlimited.

12b. DISTRIBUTION CODE

13. ABSTRACT *(Maximum 200 words)*

An investigation was conducted to experimentally quantify the interaction of particulates with the fuel-rich plume flowfield typical for solid propellant rocket motors. This was done in order to optimize enhanced mixing devices or chemical-additive addition for afterburning suppression. Laser sheet flow visualization, sound spectra measurements, plume thermal images and particle size distribution measurements were utilized with reacting and non-reacting gaseous plumes and with the plumes from highly aluminized propellant and minimum smoke propellant. Several devices were evaluated for their effectiveness in providing increased mixing in the supersonic shear layer. It was found that the generation of axial vortices in the supersonic shear layers at the nozzle exit of rocket motors operating with characteristically high exit Mach numbers and high temperatures can enhance the mixing rates and affect the afterburning. The presence of large quantities of particulates both in the shear layer and in the plume core appears to significantly change the results obtained using enhanced mixing devices. Initial results with a ramp nozzle indicate that enhanced large-scale mixing can be provided in the presence of high particulate loadings in the plume.

14. SUBJECT TERMS

Afterburning, Enhanced Mixing Devices, Solid Propellant Rocket Motor, Supersonic Shear Layer

15. NUMBER OF PAGES

59

16. PRICE CODE

17. SECURITY CLASSIFICATION OF REPORT	18. SECURITY CLASSIFICATION OF THIS PAGE	19. SECURITY CLASSIFICATION OF ABSTRACT	20. LIMITATION OF ABSTRACT
Unclassified	Unclassified	Unclassified	UL

NSN 7540-01-280-5500

Standard Form 298 (Rev. 2-89)
Prescribed by ANSI Std. Z39-18
298-102

Approved for public release; distribution is unlimited

THE EFFECTS OF PARTICULATES ON SUPERSONIC SHEAR LAYERS AND AFTERBURNING IN FUEL-RICH PLUMES

Siwon R. Lee
Lieutenant, United States Navy
B.S., Tulane University, 1983

Submitted in partial fulfillment of the
requirements for the degree of

MASTER OF SCIENCE IN ASTRONAUTICAL ENGINEERING

from the

NAVAL POSTGRADUATE SCHOOL
December 1995

Author: 

Siwon R. Lee

Approved by: 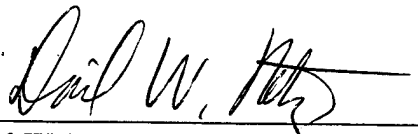

David W. Netzer, Thesis Advisor

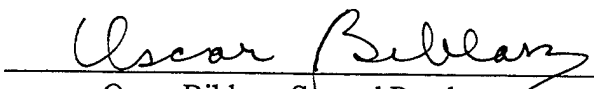

Oscar Biblarz, Second Reader

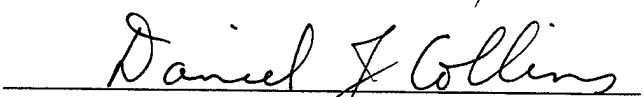

Daniel J. Collins, Chairman,
Department of Aeronautics and Astronautics

ABSTRACT

An investigation was conducted to experimentally quantify the interaction of particulates with the fuel-rich plume flowfield typical for solid propellant rocket motors. This was done in order to optimize enhanced mixing devices or chemical-additive addition for afterburning suppression. Laser sheet flow visualization, sound spectra measurements, plume thermal images and particle size distribution measurements were utilized with reacting and non-reacting gaseous plumes and with the plumes from highly aluminized propellant and minimum smoke propellant. Several devices were evaluated for their effectiveness in providing increased mixing in the supersonic shear layer. It was found that the generation of axial vortices in the supersonic shear layers at the nozzle exit of rocket motors operating with characteristically high exit Mach numbers and high temperatures can enhance the mixing rates and affect the afterburning. The presence of large quantities of particulates both in the shear layer and in the plume core appears to significantly change the results obtained using enhanced mixing devices. Initial results with a ramp nozzle indicate that enhanced large-scale mixing can be provided in the presence of high particulate loadings in the plume.

TABLE OF CONTENTS

LIST OF FIGURES

LIST OF TABLES

LIST OF SYMBOLS, ACRONYMS AND/OR ABBREVIATIONS

AP	ammonium perchlorate
Al	aluminum
C^*	characteristic exhaust velocity
CCD	charged coupled device
CFD	computational fluid dynamics
d_e	exit diameter
d_{th}	throat diameter
f	frequency
HTPB	hydroxyl terminated polybutadeine
ID	inner diameter
M_c	convective Mach number
M_{ca}	convective Mach number ambient
M_{ce}	convective Mach number exhaust
M_e	exit Mach number
P_c	chamber pressure
p_e	exit pressure
$\underline{r}$	burning rate
RDX	cyclotrimethylenetrinitramine
S_t	Stokes number
St_D	Strouhal number
T_e	exit temperature
U_a	velocity of ambient air

U_c convection velocity of large scale vortices

U_e exhaust velocity

ZrC zirconium carbide

ε area ratio

ϕ equivalence ratio

γ_e exit specific heat ratio

I. INTRODUCTION

Solid rocket propellants run generally fuel rich in order to maximize specific impulse. When the fuel rich propellant is burned large quantities of H_2 and CO are often produced in the exhaust plume. The extent to which the fuel in the exhaust plume can react with the ambient oxygen to produce afterburning depends upon the mixing rate of the plume with the environment, the altitude, the scale of the turbulence and possibly on the size distribution, surface characteristics and temperature of the exhaust particulate (which can both change the plume wave structure and act as ignition sources). Large solid rocket motors usually use aluminized propellants to increase performance. During combustion this fuel is oxidized into aluminum oxide. The aluminum oxide particles which exit the nozzle usually have a bi-modal or tri-modal size distribution [Refs. 1 & 2]. The smaller particles ($<1\mu$) are distributed almost uniformly throughout the plume. However, the larger particles ($2\text{-}30\mu$) are concentrated increasingly toward the plume centerline as their sizes increase because they cannot track the gas flow through the rapid turning at the nozzle throat. Some solid rocket motors which are used in tactical military applications have highly metallized propellants. Other tactical motors use propellants which reduce primary smoke. They generally have small amounts of condensed plume particulate from the addition to the propellant of stability additives and/or ballistic modifiers.

The particles can affect the plume thermal field [Refs. 1& 3] in various ways depending upon the altitude, particle optical properties, the number density of the

particles, the size distribution of the particles, the degree to which the particles are not in thermal equilibrium with the gases and the composition of the surrounding gases. Some specific effects of particles can be: (1) direct radiation from the particles, not only from the larger hot particles which are not in thermal equilibrium with the gases but also from smaller particles if supercooling prevents rapid solidification, (2) absorption and scattering of radiation from the gases, (3) scattering of radiation from the nozzle throat (searchlight effect) and (4) ignition sources for afterburning. In addition, high particle loadings have been shown theoretically to affect the plume near-field gas flow [Ref. 3]. Wave processes are dampened and this change in the shock/expansion wave structure can change the shape and length of the mixing layer.

The extent of afterburning in plumes can also be effected by the presence of chemical additives and/or the use of controlled mixing of the plume with the ambient air. The former has been attempted through the use of potassium salts in the case of double-base propellants [Ref. 4]. The latter has been accomplished using a variety of techniques, scalloped (petal) nozzles [Ref. 5], counterflowing nozzles [Ref. 6], ramps and wedge cutting of conical nozzles [Ref. 7], small rods [Ref. 8] or tabs [Refs. 9 & 10] inserted into the supersonic nozzle flow at the exit of the nozzle, and acoustic excitation based on flow-induced cavity resonance [Ref. 11]. The afterburning intensity can be increased or decreased depending on the physical mechanism present. In the presence of large-scale cold flow entrainment a reduction in intensity appears to be a consequence of quenching. An increase in intensity appears to stem from improved fine-scale mixing [Ref. 12].

The balance between the competing physical mechanisms of large-scale and fine-scale mixing can be affected by controlling/tailoring the mixing rates of supersonic shear layers to rapidly cool the plume using large-scale vortices while at the same time preventing fine-scale mixing of fuel and oxygen, thus reducing the extent of afterburning. To date, studies of these controlled mixing techniques have been accomplished with gases or with gases in the presence of submicron particles such as soot. The current status of mixing enhancement in supersonic free shear flows has recently been reviewed by Gutmark, Schadow and Yu [Ref. 13]. Many of the techniques reviewed are not practical for typical exhaust nozzle conditions of solid-propellant rocket motors. For tactical motors M_e= 2-4, exit pressures are typically 1-3 atm, temperatures higher than 2500 K can exist and high concentrations of condensed particulate can be present. It should also be noted that current CFD codes are not capable of accurately predicting the effects of the controlled mixing techniques.

Most efforts to date have concentrated on the effects of the gas flow on the particles rather than vice-versa. The theoretical work of Kennedy and Kollman [Ref. 14] has shown that turbulent shear stresses have negligible impact on the prediction of the rate of dispersion of particles. The expected effect of fluid motion on the particle behavior is generally determined by the magnitude of the Stokes number (S_t) [Refs. 15 & 16], a ratio of a particle inertial time scale to a fluid eddy time scale. According to Glawe and Samimy [Ref. 16], when $S_t<<1$ the particles follow the fluid motion. With $S_t\approx1$ particles are trapped by the vortices and can be dispersed more than the fluid. For $S_t>>1$

particles flow independent of fluid motion. Glawe and Samimy have also shown that incompressible flows or low compressibility in mixing layers can better entrain and disperse particles. At moderately high convective Mach numbers (e.g., 0.86) particles were observed to be unaffected by the large scale, 3-D structure of the fluid. From another viewpoint, Dash [Ref. 3] and others have used the plume codes to show that high concentrations of particulates which are not in equilibrium with the gas can significantly change the plume flowfield and thermal structure.

In the context of the present discussion a question that arises is whether or not the particle size distributions present in the plume will change the plume wave structure and thermal field and/or the mixing process induced by enhanced mixing devices. A second question is whether the large hot particles in the central region of the plume, which are little effected by the shear layer mixing, can cause afterburning ignition when the enhanced mixing devices would otherwise prohibit/reduce its occurrence. Both of these effects would require that the design of enhanced mixing devices be tailored to account for the presence of the particulate.

The overall objective of the effort at the Naval Postgraduate School is to experimentally quantify the interaction of particulates with a fuel-rich-plume flowfield typical for solid-propellant rocket motors in order to optimize enhanced mixing devices or chemical additive addition for afterburning suppression. This initial effort has been directed at determining whether or not plume particulates under typical rocket motor nozzle exit conditions can change the results obtained from devices used for enhanced

mixing in supersonic shear layers which have been reported successful in gaseous plumes for reducing the extent of afterburning.

II. EXPERIMENTAL METHOD

In this study three types of devices for enhanced mixing of supersonic flow were considered, tabs in the flow at the nozzle exit plane, annular cavities placed at the exit plane, and contoured ramps placed in the nozzle. Initially only the tabs and the cavities were investigated. The effectiveness of these devices for significantly changing the extent of afterburning was first evaluated by exhausting hot, fuel rich, supersonic gaseous flows into the atmosphere and recording the plume temperature distribution using a thermal imaging camera. Those devices found to be most effective for changing the afterburning behavior were then subjected to laser-sheet flow visualization in non-reacting flows to examine the resulting effects on mixing and/or jet spreading rate. The noise spectrum produced by each device was also recorded. Finally, the devices found to produce the largest change in afterburning were used in an exhaust nozzle of a solid-propellant rocket motor, using both aluminized and minimum smoke solid-propellant to determine the plume particulate effects on the mixing process/afterburning. Subsequently, the contoured ramps were investigated using the laser sheet flow visualization and motor firings.

The laser sheet used for flow visualization was provided by an 8 watt argon-ion laser as shown in Figure 1. The time averaged effects of the mixing devices were observed using a Nikon F-801S camera with 1600 ASA color film and a Xybion ISG-350, electronically gated, intensified CCD video camera. The noise spectra were measured using a Larson-Davis Laboratories Model 2530 microphone and preamplifier and recorded

at a sampling rate of 1 MHz. The data analysis capabilities of the VIEWDAC PC software were utilized to produce the power spectra.

For reacting flow measurements (gases and solid-propellant motors) the afterburning characteristics were recorded using an AGEMA 870 thermal imaging camera with a wavelength band of 3.5-5.0 μ. The particle size distributions were made with a Malvern 2600 particle analyzer with a 100mm Fourier transfer lens.

The motor geometry was similar for all phases of the investigation. A small (5.1cm ID) solid-propellant workhorse motor case was modified to permit gaseous injection and to provide an ignition source as shown in Figure 2. For flow visualization with the laser sheet, ethanol was injected into the hydrogen port with a tube atomizer and air was injected into the nitrogen port. When operated as a solid-propellant motor an internally and one-end-burning grain was utilized for most tests as shown in Figure 3. One test was conducted using an end-burning geometry. The propellant characteristics are given in Table 1.

Propellant	PS-1	X
Nominal Composition	AP 70% Al 20% HTPB 10%	AP 82 % R45M 11% RDX 4% Dioctyl Adipate 2% ZrC 1%
Density (gm/cc)	1.84	1.73
C^* (m/s)	1557	1526
$\underline{r}$ (cm/s)	$0.541\ P_c(MPa)^{0.376}$	$0.048\ P_c(MPa)^{0.248}$
M_e	3.15	2.14
T_e (K)	2755	2198
γ_e	1.12	1.14
u_e (m/s)	2231	1946
ϕ	1.33	1.31
ε	4.00	2.31
p_e (MPa)	0.119	0.143

Table 1. Solid Rocket Motor Propellant Characteristics for Standard Nozzles With and Without Exit Tabs and Cavities

Tactical motors often use underexpanded exhaust nozzle flow. However, large boosters operate under a changing expansion condition, including ideal expansion. In addition, the cavity devices used by Yu and Schadow had ideally expanded flows [Ref. 11]. For this reason, the present investigation was initiated using ideally expanded flows. Solid-propellant rocket motors usually operate at high pressures. For realistic combustion and nozzle flow the chamber pressure should be ≥ 2 MPa. Expanding to atmospheric pressure therefore results in higher exit Mach numbers than reported by Yu and Schadow in their investigation of cavity-excited vortex enhancement [Ref. 11].

The fuel-rich, high temperature exhaust gases were produced using the characteristics shown in Table 2. The nozzle exhaust was into static air (U_a = 0). Assuming no shocks in the shear layer permits the convective Mach number to be determined [Ref. 11].

P_c MPa	P_e MPa	d_{th} cm	d_e cm	U_c m/s	T_e K	γ_e	ϕ	M_e	M_{ce}	M_{ca}
2.07	0.108	0.508	1.1016	723	1600	1.26	2.0	2.7	2.06	2.09
where: $M_{ce} = (U_e-U_c)/a_e$; $M_{ca} = (U_c-U_a)/a_a$; M_c = Convective Mach number; U_c = convection velocity of large scale vortices; U_a = 0 [Ref. 11].										

Table 2. Fuel-Rich Exhaust Gas Characteristics (H_2, O_2, N_2).

The 360° cavities used in an attempt to enhance the shear layer followed the work performed by Yu and Schadow [Refs. 11 & 13]. Using a Strouhal number of approximately 0.5 ($St_D = f\ d_e/U_e$) yields the preferred mode frequency. The cavity geometries shown in Figure 4 were utilized in an attempt to produce the desired frequencies.

The tabs employed at the exhaust plume were scaled using the results reported by Ahuja and Brown [Ref. 8] and are shown in Figure 5. The contoured ramp nozzle is shown in Figure 6.

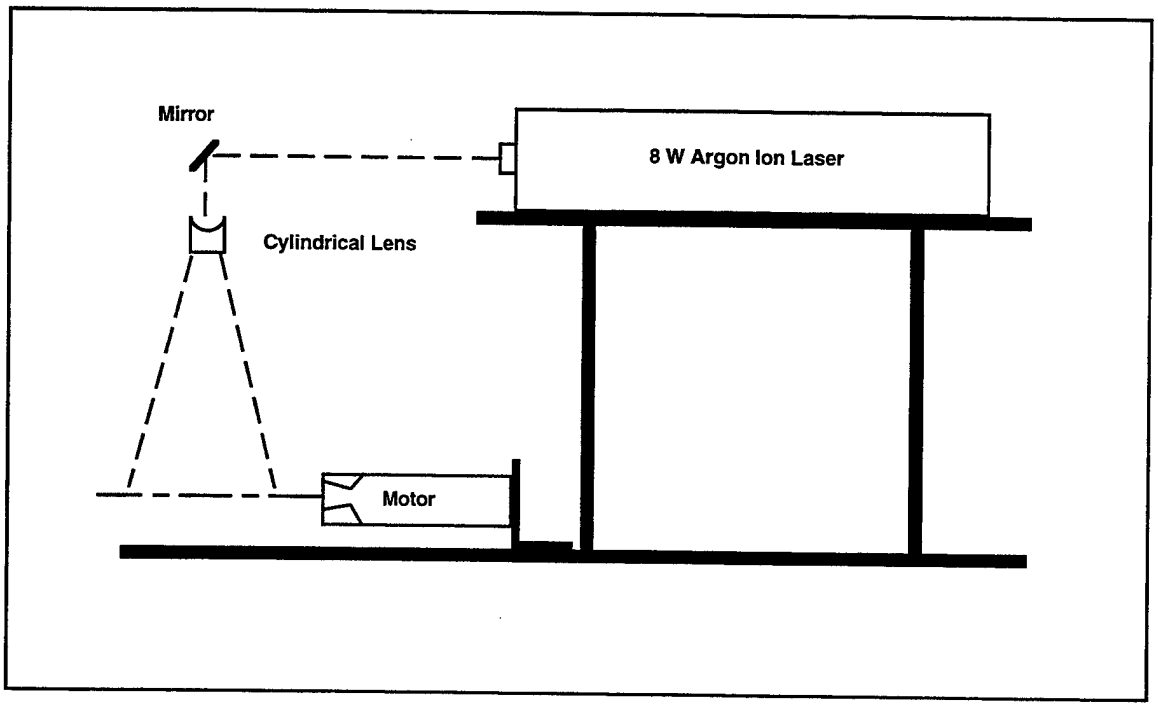

Figure 1. Schematic of Laser-Sheet Flow Visualization Set-Up

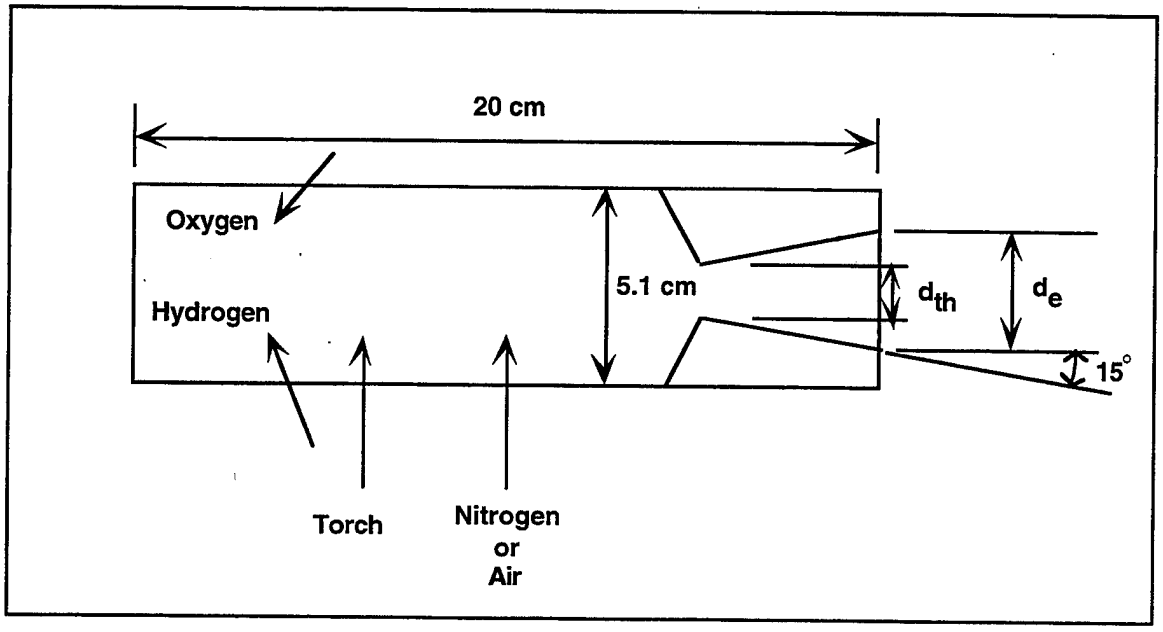

Figure 2. Schematic of Test Motor

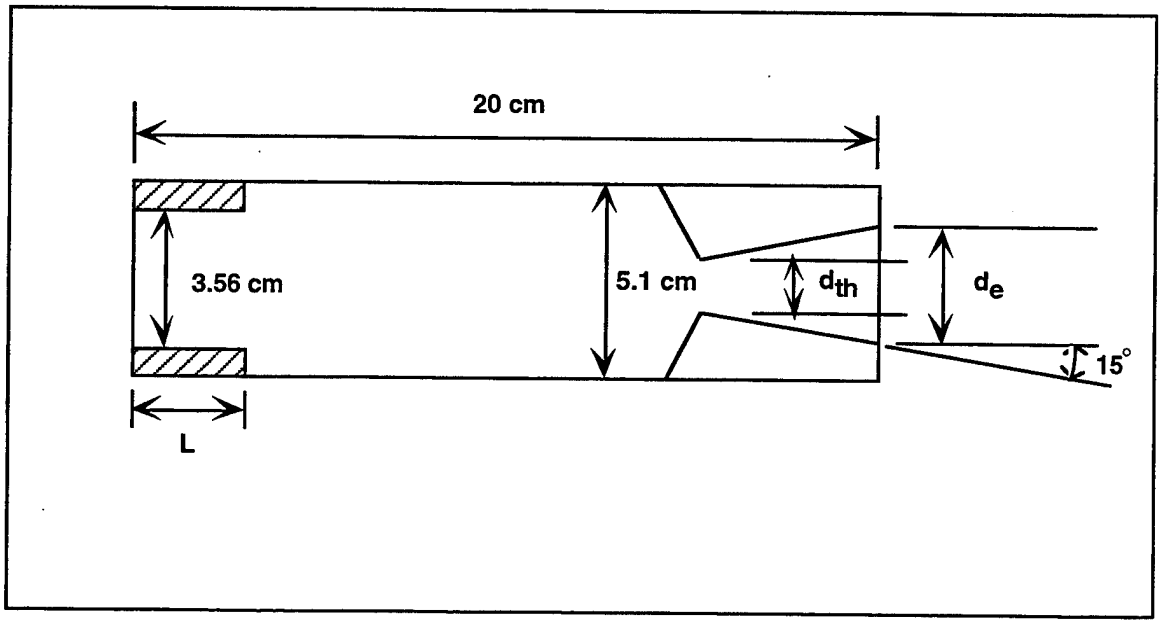

Figure 3. Schematic of Solid-Propellant Motor

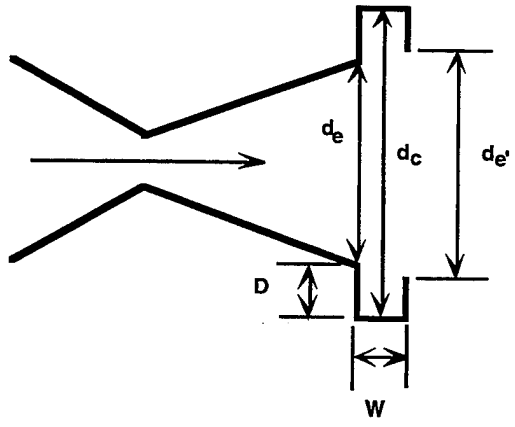

	D	W	d_e	d_c	$d_{e'}$
A	0.889	1.016	1.016	2.794	1.016
B	0.254	1.016	1.016	1.524	1.016
C	0.889	0.508	1.016	2.794	1.016
D	0.508	0.508	1.016	2.032	1.016
E	0.254	0.508	1.016	1.524	1.016
F	-	1.016	1.016	1.656	1.321
G	-	0.508	1.016	1.656	1.321

Figure 4. Schematic of 360° Cavities

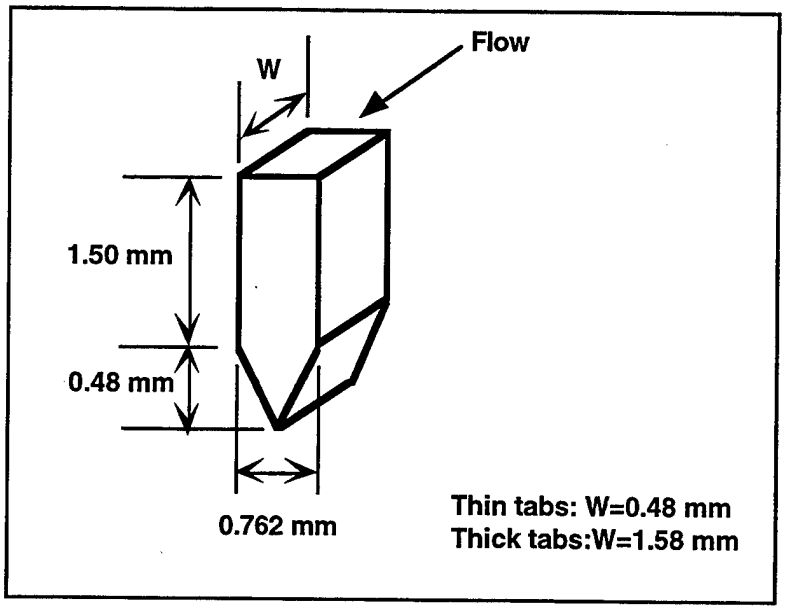

Figure 5. Schematic of Exhaust Tabs

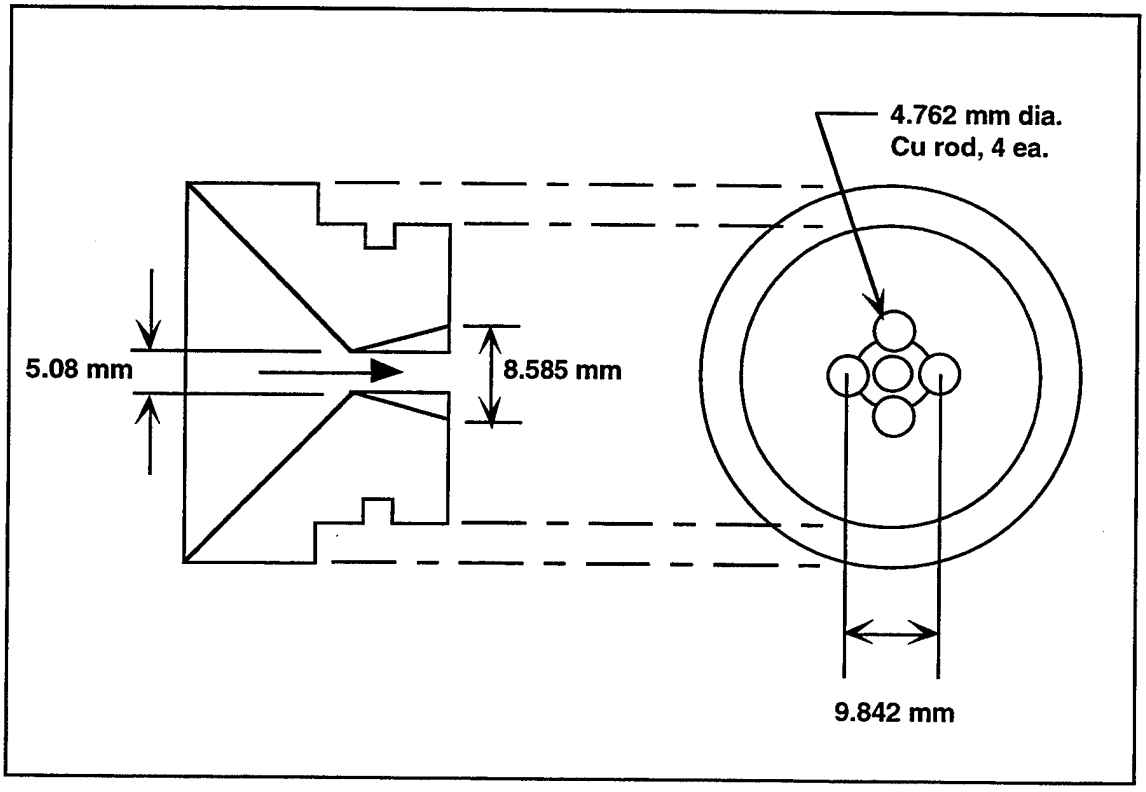

Figure 6. Schematic of Contoured Ramp Nozzle

III. DISCUSSION AND RESULTS

A. INVESTIGATION OF NOZZLE EXIT TABS AND CAVITIES

The reacting gas flows showed that only one of the devices investigated was capable of significantly changing the afterburning characteristics under the motor operating conditions employed, the thick (1.58 mm) tabs located 180° opposed at the nozzle exit. Long exposure laser sheet photographs are presented in Figure 7 which show that the thick tabs increased the rate of mixing and jet spreading. Laser sheet photographs of thin tabs and cavities as seen in Figure 8 showed no significant effects on the plume. Detailed plume structure cannot be seen in these figures due to the time averaged effects resulting from the slow shutter speed of the conventional film camera. An attempt was made to obtain images of the plumes through the use of the Xybion camera which has an electronically gated shutter. It was determined that the existing laser light source did not have sufficient intensity to provide illumination at the short exposure times required. Thermal images shown in Figures 9 & 10 also illustrate the increase in the rate of mixing and jet spreading obtained with the thick tabs. Figure 11 shows the average (from two representative thermal images) plume centerline temperature profiles, assuming an effective emissivity of 0.1. These figures show that the axial vortices generated by the tabs increased the mixing rate, which in turn resulted in both an increased maximum temperature and a peak centerline temperature further upstream. The tabs shifted the peak temperature position from approximately 27 d_e to approximately 20 d_e. However,

the total radiation from the plumes were not significantly different. Thus, the tabs enhanced the fine-scale mixing without providing adequate large-scale vortices for quenching. The plume centerline temperature profile in Figure 11 indicates the possible existence of a shock immediately downstream from the nozzle exit plane when the tabs were present. Another interesting result from the thermal images was that the afterburning was unsteady for flows with and without the tabs. The fluctuations in afterburning occurred at a very low frequency of approximately 5 Hz. It is not clear at this point whether this was a plume generated phenomena, a result of the unsteady flow/interaction characteristics within the side-dump combustor or a result of motor body, motor base and plume interactions.

A total of 7 cavities were investigated to determine if large scale mixing could be generated by acoustic resonance. Each cavity was affixed to the test motor at the exit plane of the standard nozzle. Initially, cavities A through E as shown in Figure 4 were analyzed. Analysis of laser sheet flow and thermal images revealed some fine-scale mixing effects but no large-scale mixing. In order to reduce the effect of the cavity lip on the expanding plume a cavity device was modified to enlarge the downstream orifice. Despite this modification no large-scale mixing effects were noted.

In addition, the sound recordings taken during the non-reacting gas experiments showed that no dominant frequencies were produced by the cavities, a result consistent with the plume thermal images. This was not unexpected since as convective Mach

number increases the jets become more stable with the suppression of the vortex pairing process. The compressible shear layers also exhibit much reduced spreading rates.

In order to determine if the presence of particulate matter in the plume could affect the shear layer mixing and/or the augmented mixing generated by the tabs in gaseous flows, motor firings were conducted using a highly-aluminized propellant (PS-1), and a minimum-smoke propellant (X). Runs were made with and without tabs. Peak combustion chamber pressures for all runs were between 1.86 and 2.00 MPa (270-290 psia). A representative pressure-time trace is shown in Figure 12. Post-firing examination of the tabs used for both propellants revealed erosion on their upstream surfaces, but the tab height and downstream cross-sections were not deteriorated.

For the PS-1 propellant firings approximately 38% of the mass exiting the nozzle was contained in condensed particulate. Malvern measurements [Ref. 17] across the plume, as seen in Figure 13, showed that most of the volume (mass) of the particulate was in particles with diameters between 4 and 5.5 μ. However, practically all of the number of particles had diameters smaller than 1.9 μ. Particles larger than approximately 4 μ can be expected to be concentrated along the center of the plume in a cylinder with a diameter approximately that of the throat diameter. This results from the larger particles being unable to make the turn with the gas through the nozzle throat. However, the small particles (<1μ) will follow the gas flow quite well in the supersonic flow and be distributed nearly uniformly throughout the plume. These small particles will be present in the supersonic shear layer at the nozzle exit plane. Utilizing the measured particle

sizes, calculated convective velocities in the shear layer and estimates of the shear layer thickness as provided by Yu and Schadow [Ref. 12 & 13], values of the Stokes number range from 0.4 - 21. Thus, the path of the particulates within the mixing layer are expected to be affected by the presence of any large scale vortices introduced under typical rocket motor nozzle conditions. The high concentrations of particulate which are not in equilibrium with the gases are also expected to affect the flow structure and thermal field in the plume.

The plume temperature profiles for the highly aluminized propellant (Figure 14) and thermal images (Figures 15 & 16) indicated that the tabs did not shift the peak temperature upstream or increase the peak temperature from afterburning as they did for the particle free exhaust flow. In fact, significant afterburning was not evident. This may have been a result of the motor firings having an equivalence ratio of 1.33 vs. 2.0 for the gaseous flow (although exhaust temperature was much higher for the motor firing), or the plume radiation may have been dominated by the particles. In either case it is apparent from these tests that devices effective for changing the mixing rates and afterburning in supersonic gaseous flows may not be effective when large quantities of particles are present. In a further attempt to quantify the effects of the tabs, a single thick tab was placed at the exit plane of a standard nozzle at the 12 o'clock position, as shown in Figure 17, in order to obtain laser sheet flow visualization photographs of the tab and no tabs conditions simultaneously. Due to the time averaged effects caused by the relatively

long exposure time of the film camera it was difficult to ascertain if the tab had a significant effect on jet spreading in Figure 18.

Propellant X, a minimum smoke propellant, was used in firings with and without tabs to determine if the these devices would be effective in changing mixing and afterburning in the exhaust plume. As seen in Figure 19, the presence of tabs corresponded with a slight shift in the location of the peak centerline plume temperature as compared with the standard nozzle. This result was not as pronounced as that encountered in the reacting gas flow experiment. Overall shape of the centerline peak temperature plot reveals a rapid drop in temperature in both cases. Analysis of the results of these firings, which occurred at an equivalence ratio of 1.31, indicates a weak afterburning condition existed. At this equivalence ratio it is possible that exhaust plume cooling found under normal exhaust flow conditions existed. Figure 20 shows that the particle volume (mass) distribution was in particles with diameters of <2 to 20 μ and all the number of particles were smaller than 4 μ. It should be noted that Malvern data derived from firings of a zirconium carbide propellant can be inconsistent from firings of an aluminized propellant. Analysis of the combustion and exhaust temperatures encountered with this propellant indicates that the zirconium carbide particles in the propellant may not have been completely oxidized. Thus, some of the non-spherical ZrC particles may have been present in the plume. These non-spherical particles would cause the particle sizing results from the Malvern observations to be inaccurate.

B. INVESTIGATION OF CONTOURED RAMP NOZZLE

An existing nozzle was modified in order to create contoured ramps in the nozzle. The ramps begin at the nozzle throat and protrude into the nozzle forming a cruciform shaped orifice at the exit plane. The exit area ratio of the original nozzle was 2.86 and after modification was reduced to 1.85, resulting in underexpanded nozzle flow as shown in Table 3. In the firings involving propellant X, an end burning grain configuration was used in order to achieve near ideal nozzle expansion conditions.

	P_c	P_e	d_{th}	d_e	ϕ	M_e	T_e	γ_e
	MPa	MPa	cm	cm			K	
PS-1	2.69	0.403	0.51	0.94	1.33	1.94	3028	1.12
X	1.03	0.148	0.51	0.94	1.31	1.95	2316	1.14

Table 3. Nozzle Exit Conditions With Contoured Ramp Nozzle

The laser sheet photograph of the contoured ramp nozzle in Figure 21 in non-reacting flows shows a rate of mixing and jet spreading similar to that encountered with the opposed thick tabs. The contoured ramp nozzle was used in a firing with aluminized propellant in a radial burning grain configuration. The exhaust plume centerline temperature profile in Figure 22 had a distinct maximum at approximately 10 exit diameters, similar to the profile obtained previously for the thick tabs with the minimum smoke X propellant (Figure 19). This was, however, different from the PS-1 propellant results with thick tabs (Figure 14). In addition, the plume centerline temperatures for the

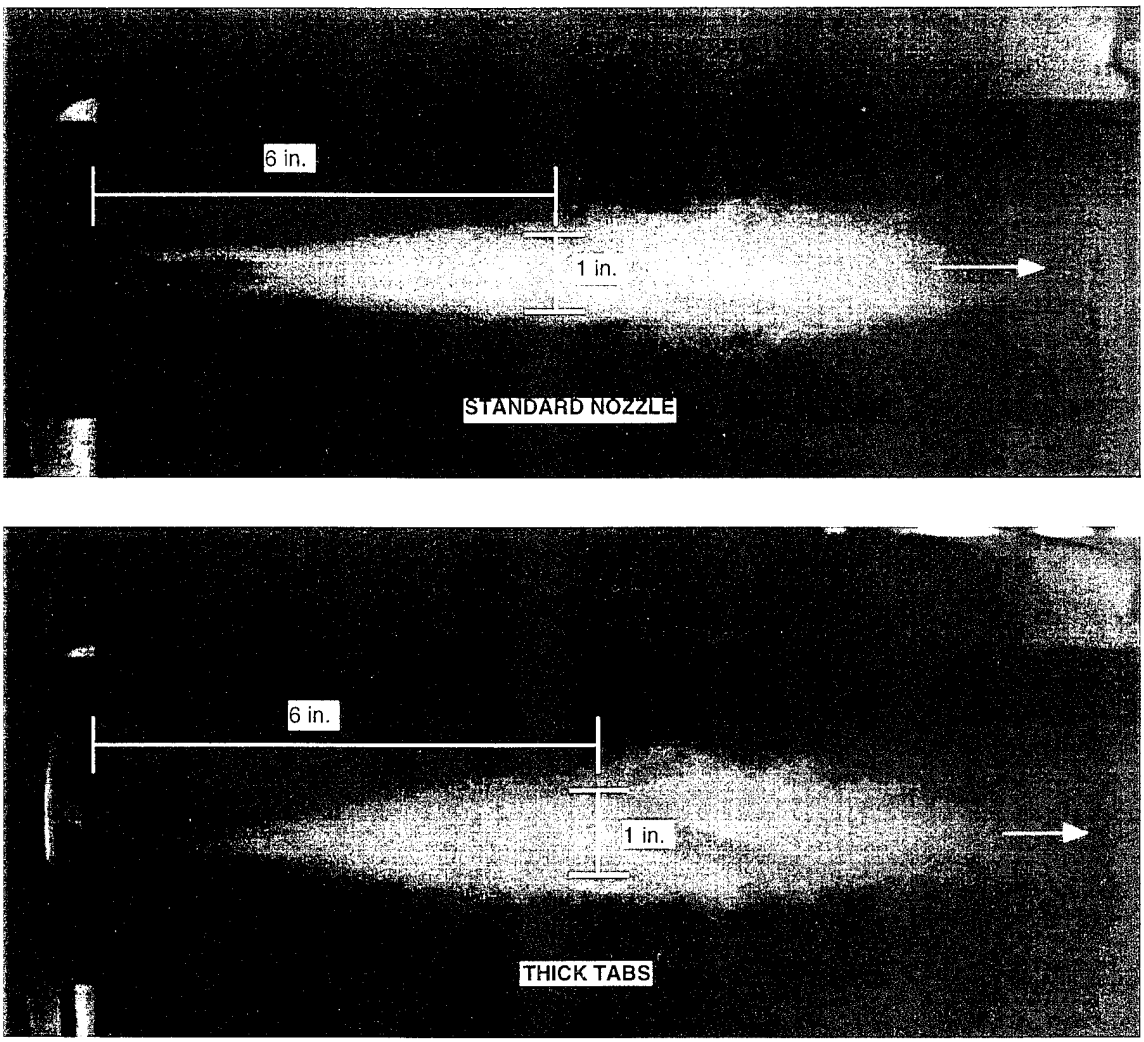

Figure 7. Laser Sheet Flow Visualization of Non-Reacting Flows With and Without Enhanced Mixing Devices

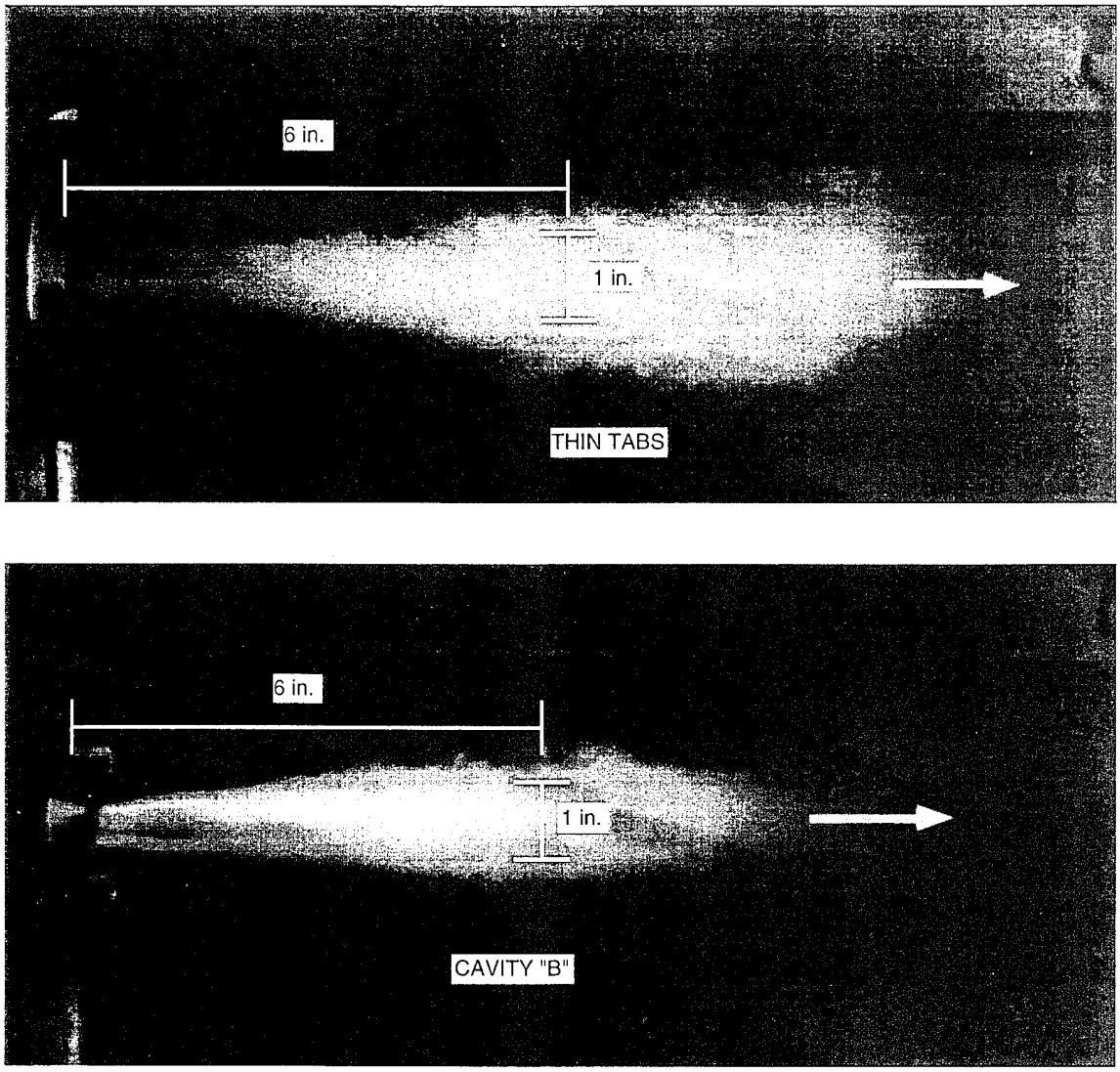

Figure 8. Laser Sheet Flow Visualization of Non-Reacting Flows With Enhanced Mixing Devices

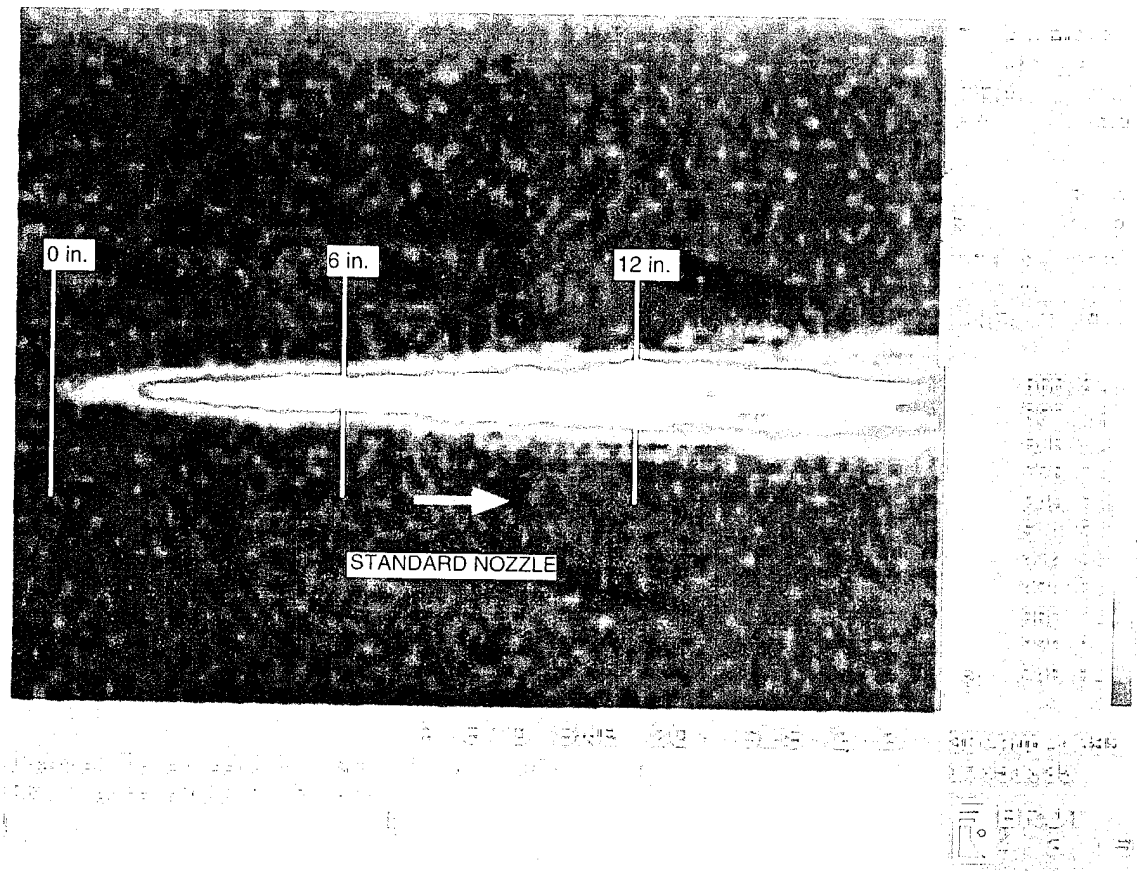

Figure 9. Thermal Image of Plume From Fuel-Rich Gaseous Reactants Using Standard Nozzle

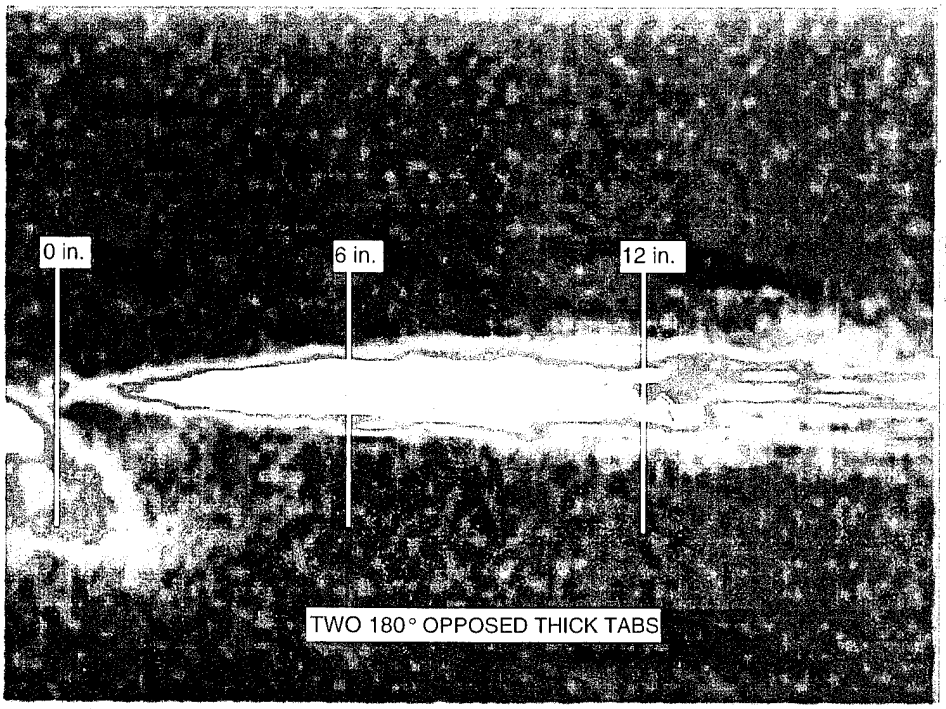

Figure 10. Thermal Image of Plume From Fuel-Rich Gaseous Reactants Using Thick Tabs

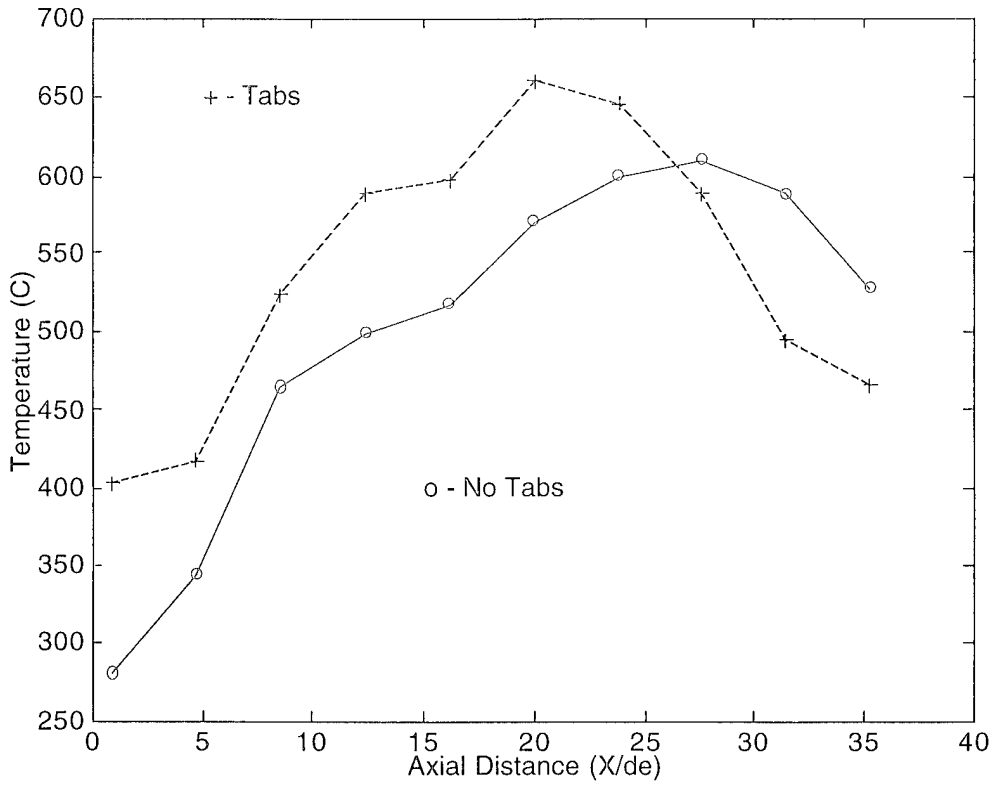

Figure 11. Exhaust Plume Centerline Temperature Profiles from Fuel-Rich Gas Combustion (emissivity = 0.1)

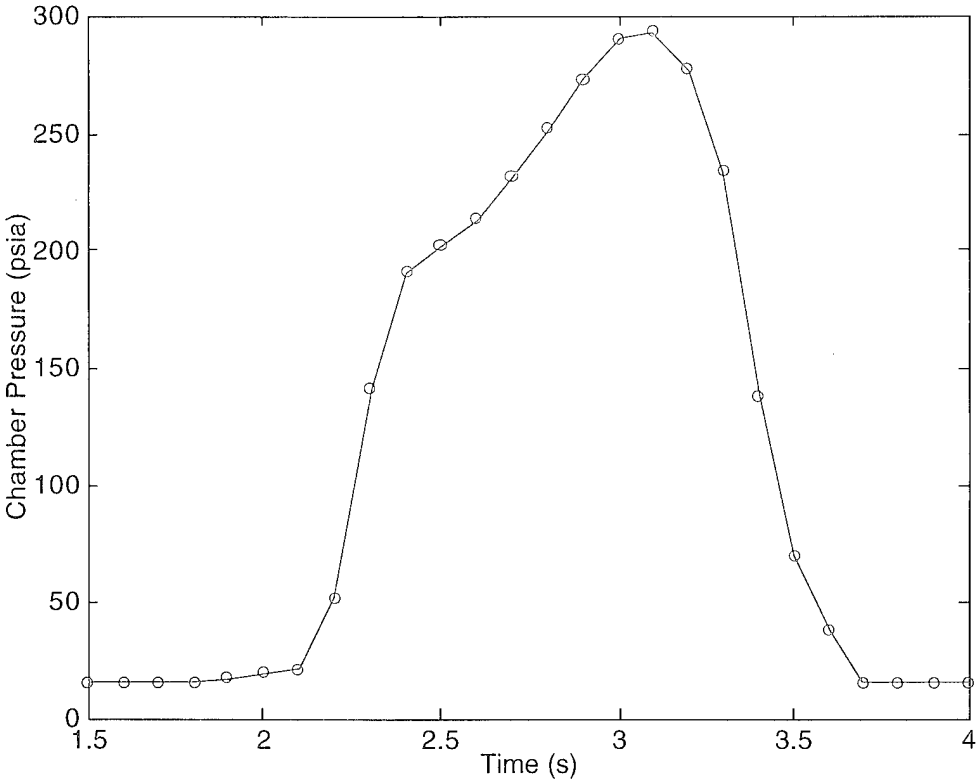

Figure 12. Pressure-Time Trace From Solid Rocket Motor Firing

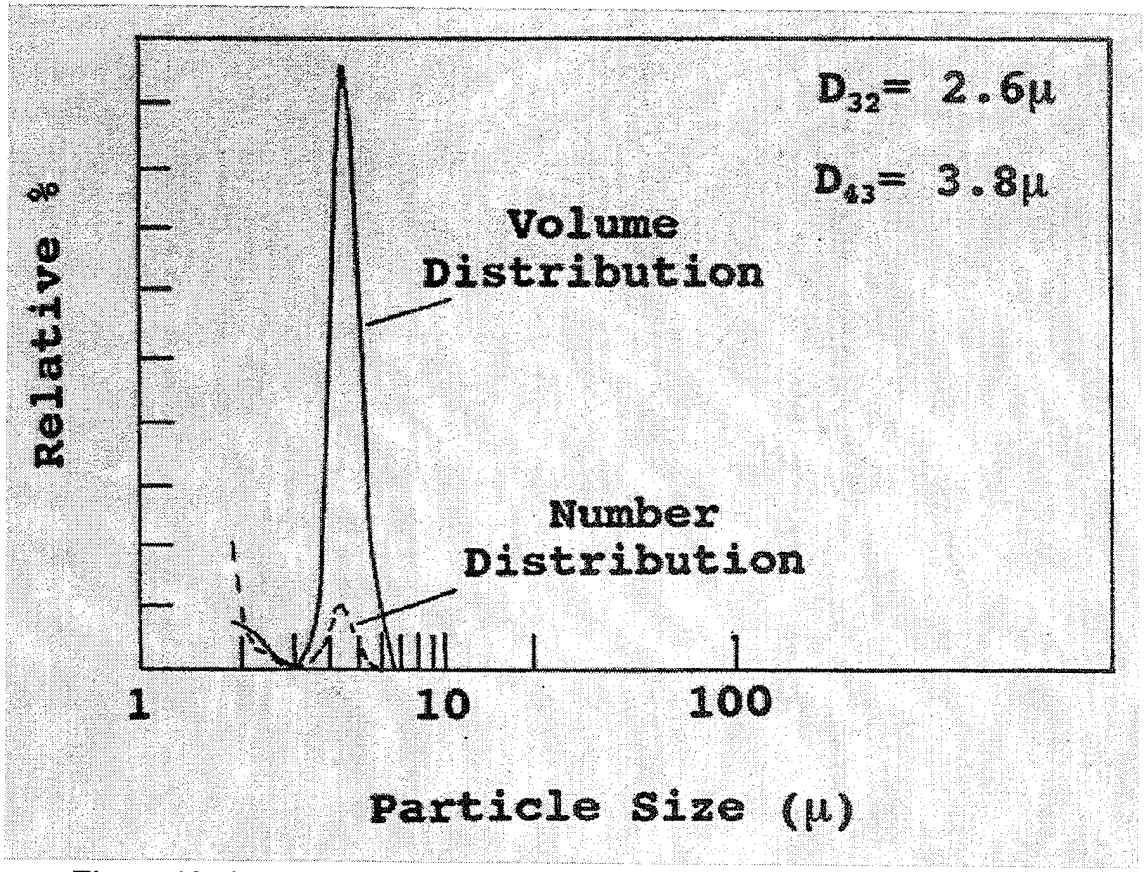

Figure 13. Particle Size Distribution in PS-1 Propellant Plume [Ref. 17]

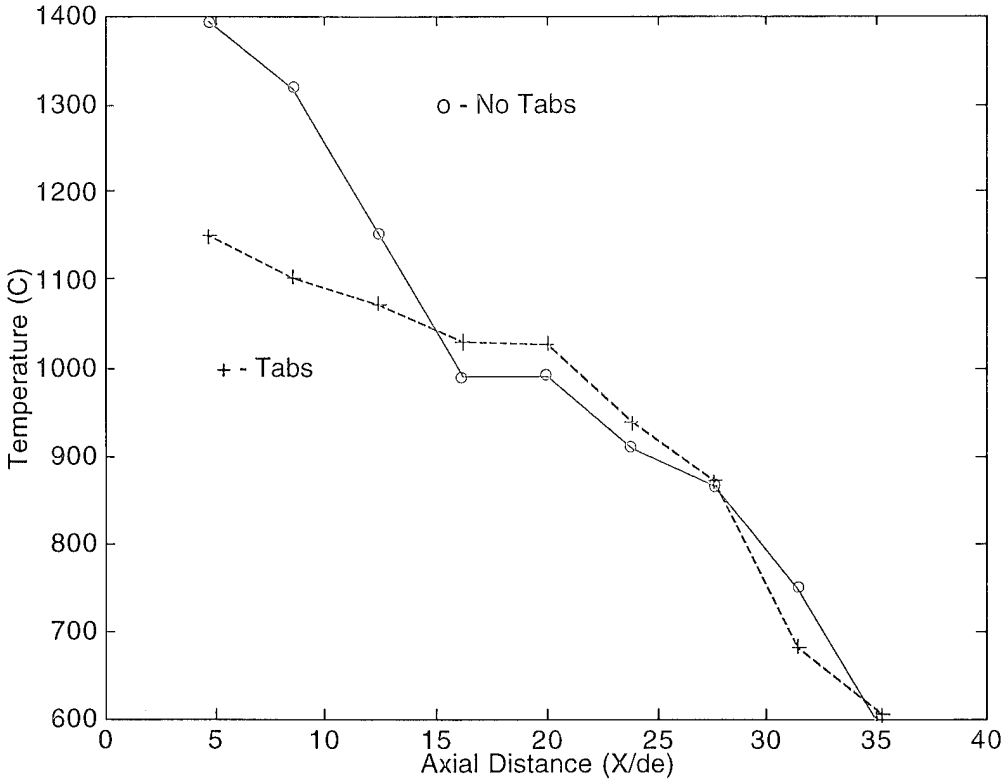

Figure 14. Exhaust Plume Centerline Temperature Profiles from Solid Rocket Motor Firings Using PS-1 Propellant (emissivity = 0.1)

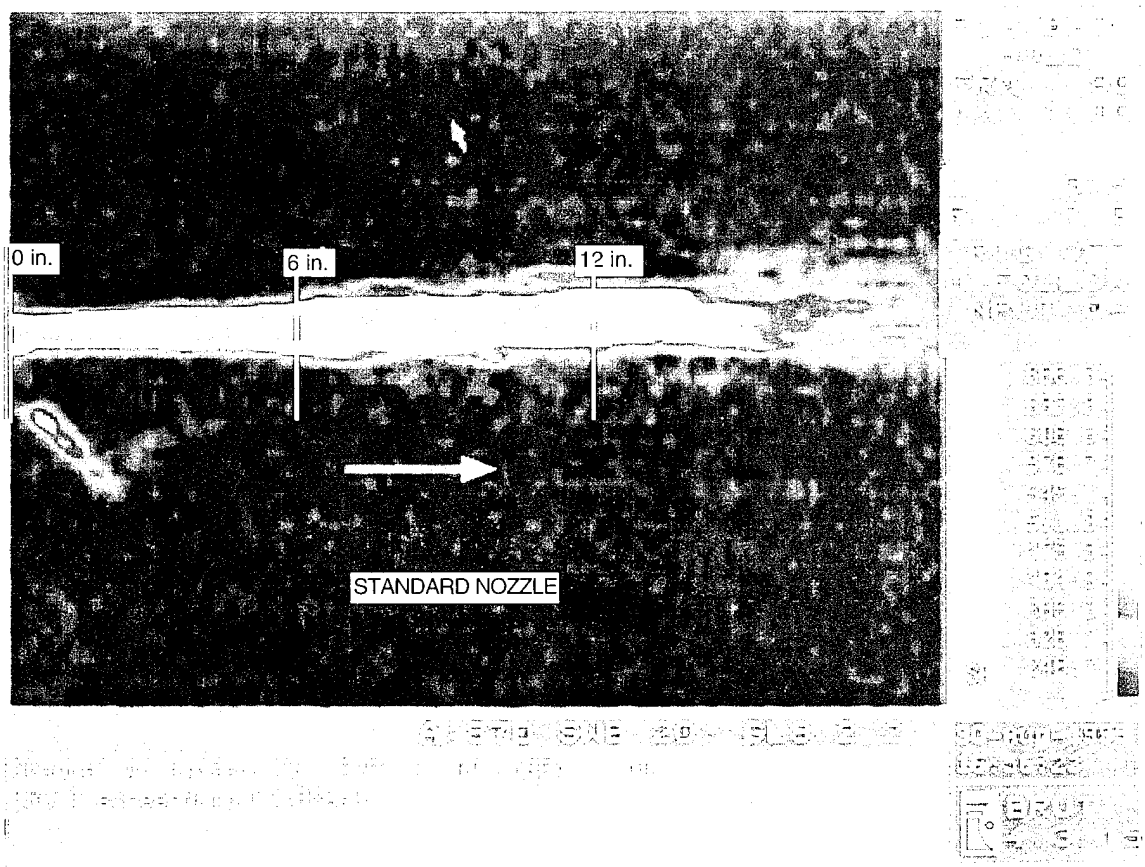

Figure 15. Thermal Image of Plume from Solid Rocket Motor Using Standard Nozzle

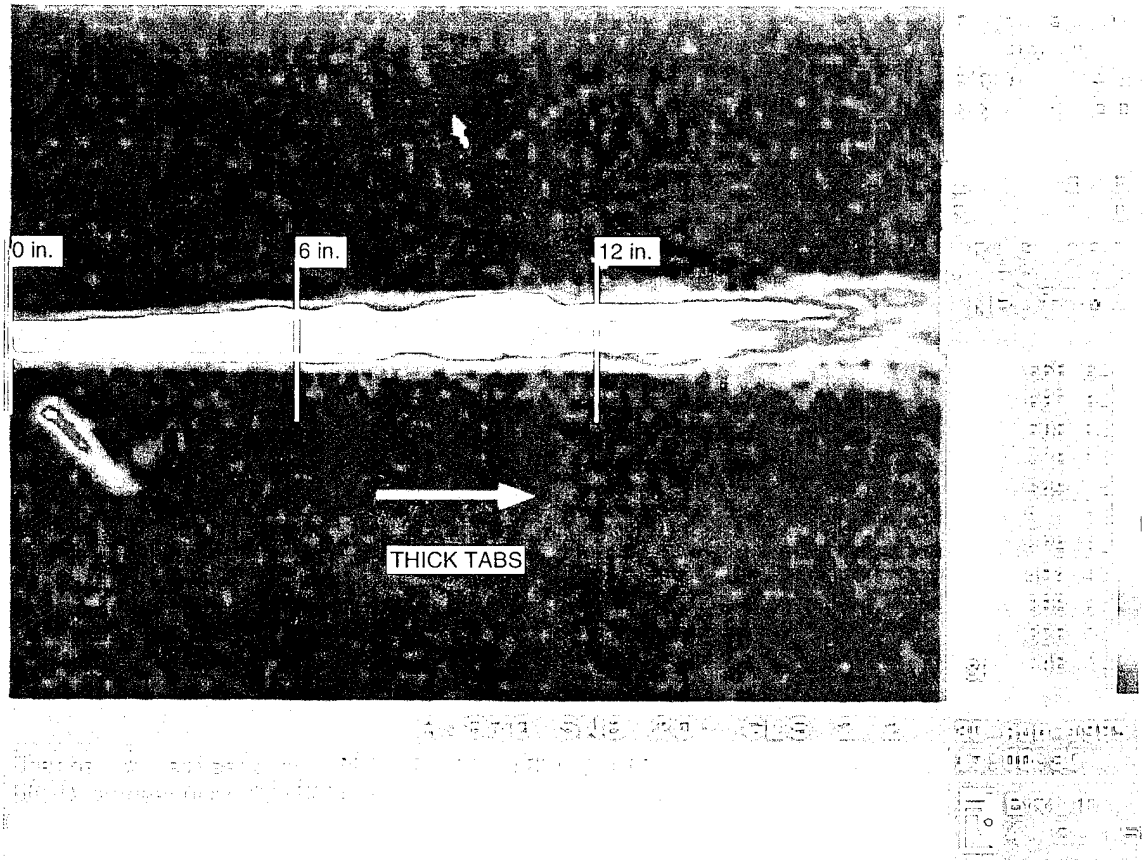

Figure 16. Thermal Image of Plume From Solid Rocket Motor Using Thick Tabs

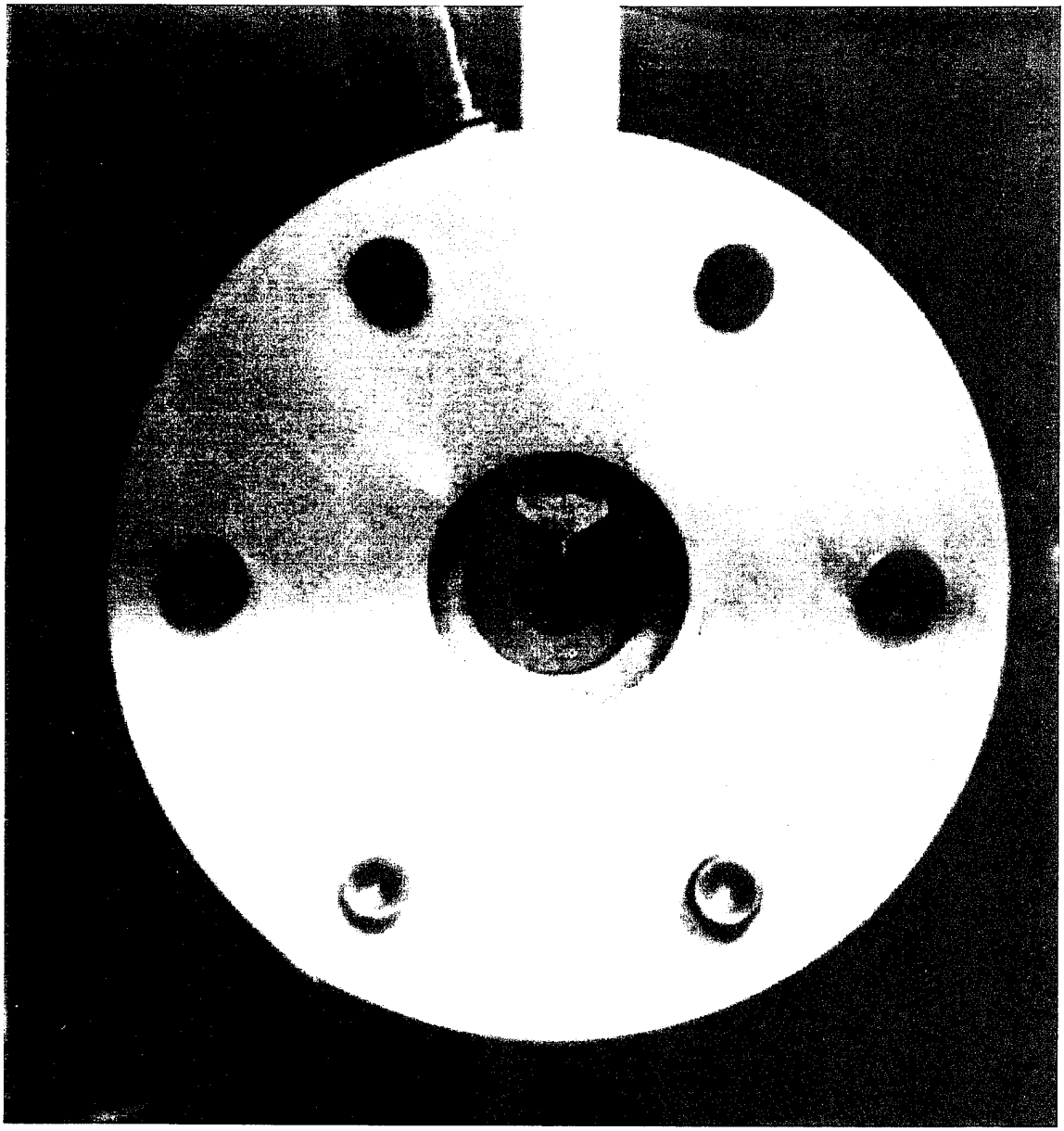

Figure 17. Photograph of Motor Nozzle with One Thick Tab Installed

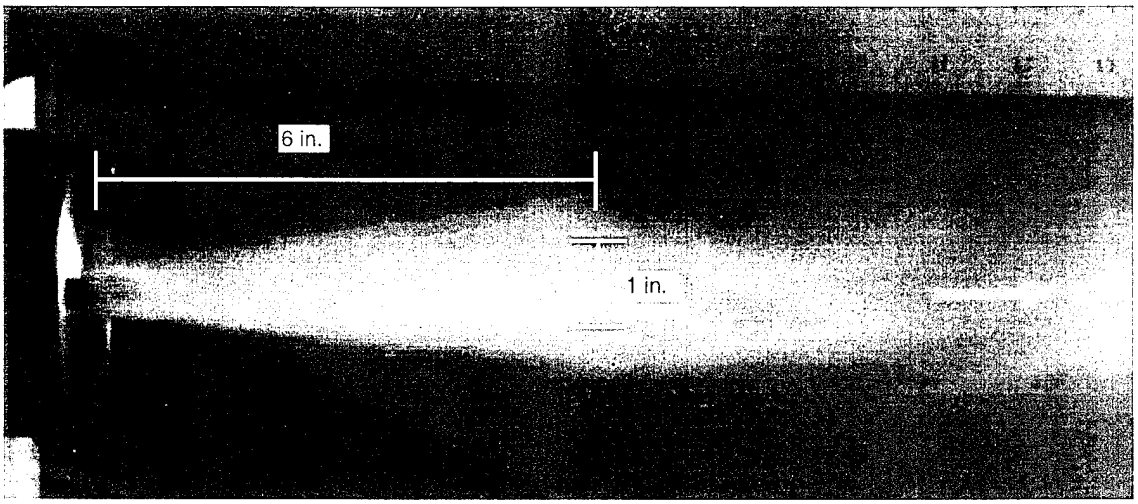

Figure 18. Laser Sheet Flow Visualization Photographs of Non-Reacting Flows With One Thick Tab

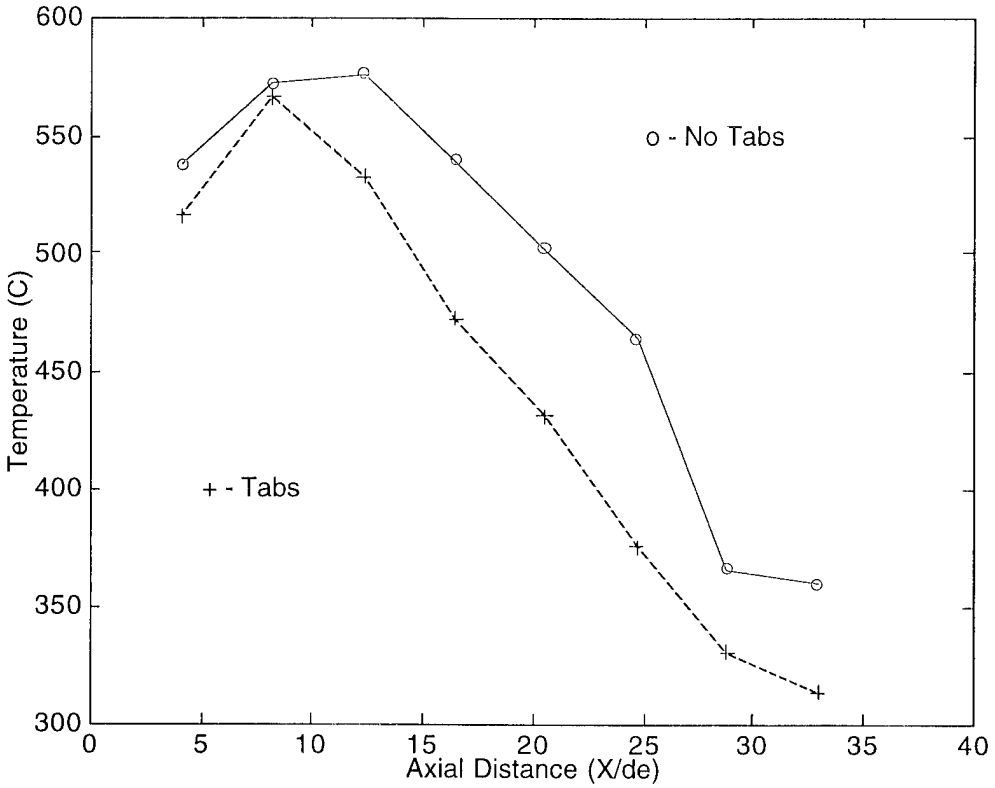

Figure 19. Exhaust Plume Centerline Temperature Profiles from Solid Rocket Motor Firings Using X Propellant (emissivity = 0.1)

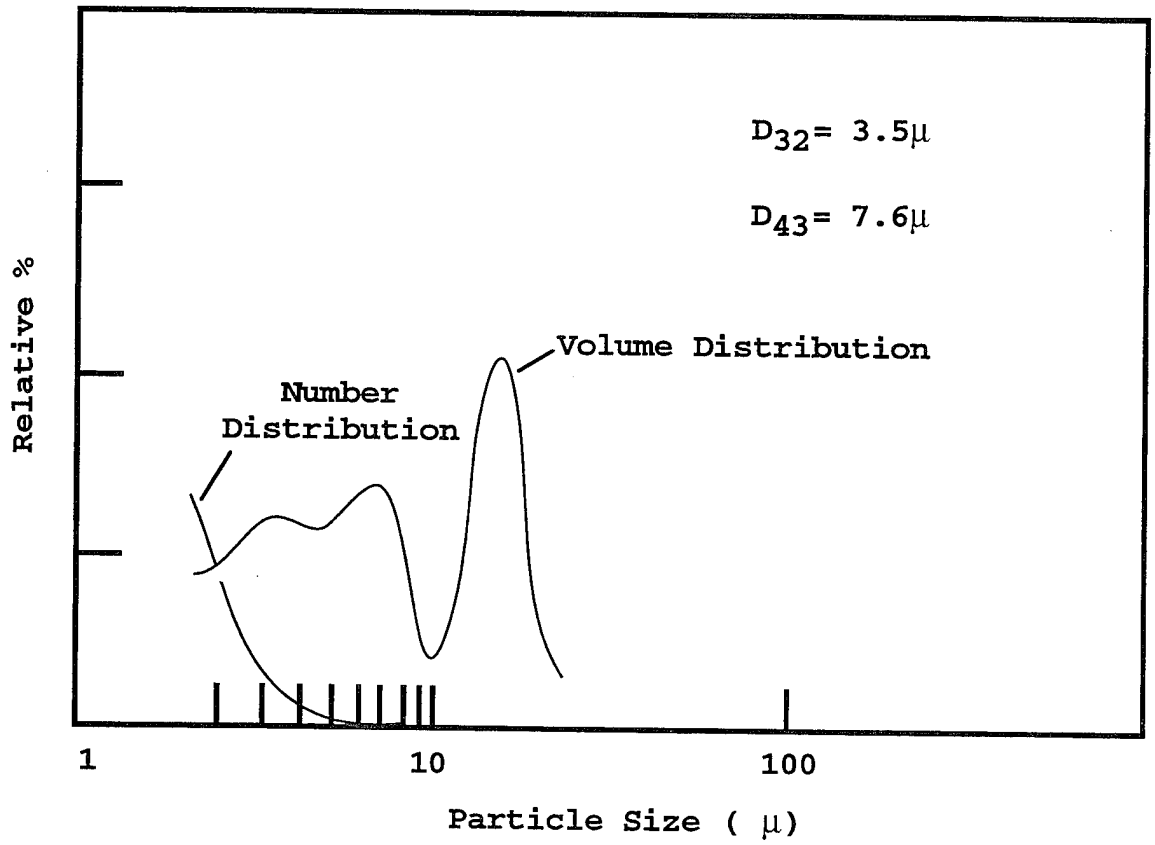

Figure 20. Particle Size Distribution X Propellant in Plume

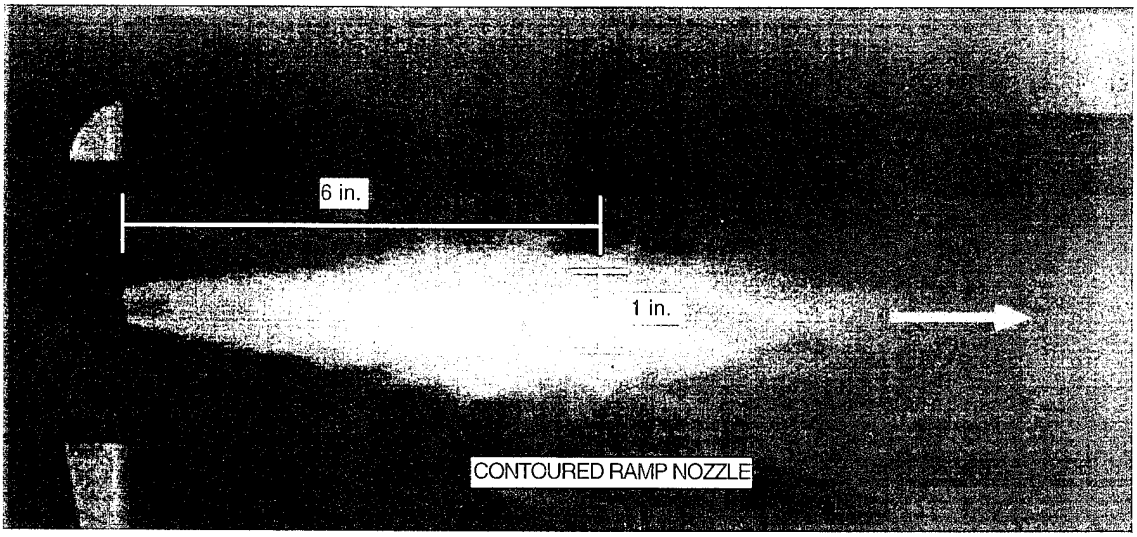

Figure 21. Laser Sheet Flow Visualization Photographs of Non-Reacting Flows With Contoured Ramp Nozzle

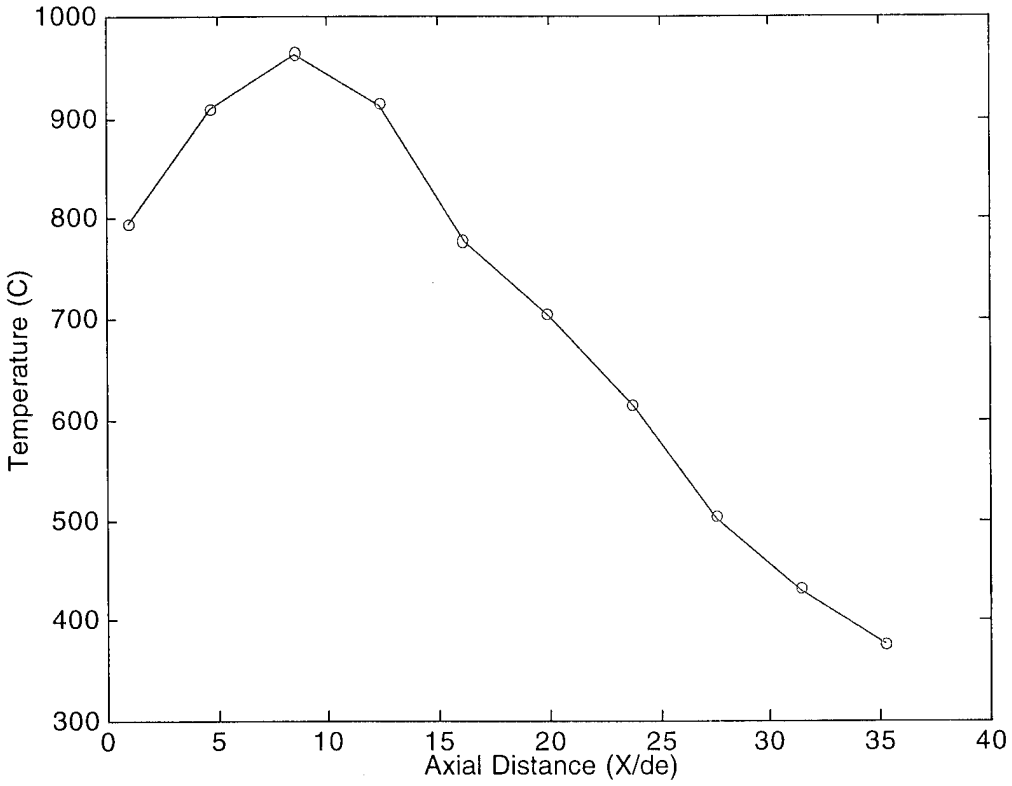

Figure 22. Exhaust Plume Centerline Temperature Profile for Solid Rocket Motor and Contoured Ramp Nozzle Using PS-1 Propellant (emissivity = 0.1)

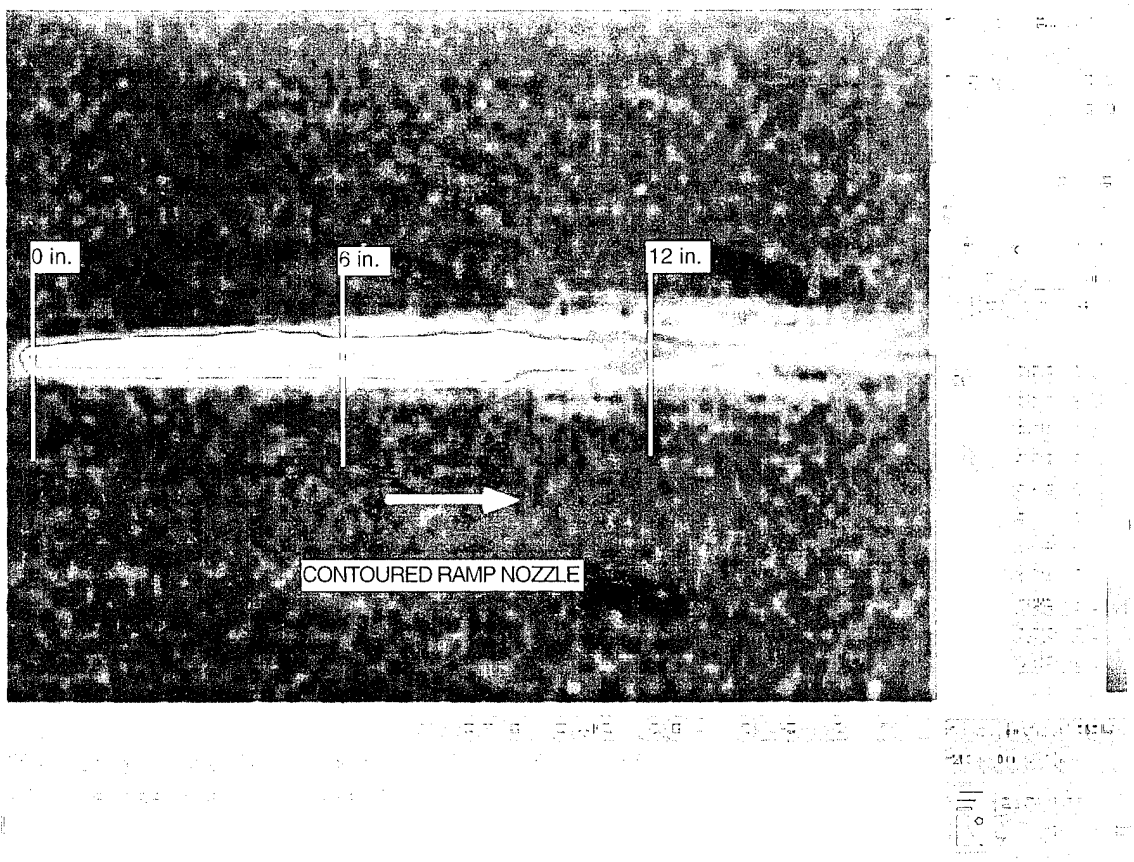

Figure 23. Thermal Image of Plume of Solid Rocket Motor

IV. CONCLUSIONS AND RECOMMENDATIONS

The generation of axial vortices in the supersonic shear layers at the nozzle exit of rocket motors operating with characteristically high exit Mach numbers and high temperatures can enhance the mixing rates and affect the afterburning for propellant flow. For example, jet vanes used for thrust vector control in tactical motors that utilize NATO class AA propellants ("smokeless") could possibly be shape-optimized to also suppress afterburning. However, initial data have shown that the presence of large quantities of particulate both in the shear layer and plume core may significantly change the plume thermal field and the results obtained using enhanced mixing devices. The contoured ramp nozzle shows promise for providing enhanced large-scale mixing in the presence of high particulate loadings, but further testing is required for validation of the initial findings.

To continue the investigation into the design of devices for providing enhanced mixing/afterburning suppression in rocket motor plumes the following are recommended:

1. Increase laser light source intensity to allow high speed photographs of at least 1/10000 second shutter speed to capture the detailed plume structure.

2. Obtain simultaneous measurements of pressure and temperature fluctuations with temperature fluctuation measurements in the plume to isolate the source of the unsteady afterburning.

3. Optimize the shapes of the enhanced mixing devices using both highly-aluminized and minimum smoke propellants to produce desired afterburning effects.

4. Conduct additional investigations to fully characterize the zirconium carbide particulates in the plume of minimum smoke propellants.

LIST OF REFERENCES

1. Laredo, D. and Netzer, D.W., "The Dominant Effect of Alumina on Nearfield Plume Radiation", Journal of Quantum Spectroscopy and Radiation Transfer, Vol. 50, No. 5, November 1993, pp. 511-530.

2. Laredo, D., McCrorie II, J. D., Vaughn, J.K. and Netzer, D.W., "Motor and Plume Particle Size Measurements in Solid-propellant Micromotors", Journal of Propulsion and Power, Vol. 10, No. 3, May-June 1994, pp. 410-418.

3. Dash, S.M., "Rocket Motor Plume Flowfield: Phenomenology and Simulation", AGARD Lecture Series 188, Rocket Motor Plume Technology, AGARD-LS-188, June 1993.

4. Smith, P.K., "Propulsion", AGARD Lecture Series 188, June 1993, pp. 1-22.

5. Narayanan, A.K. and Damodaran, K.A., "Supersonic-Ejector Characteristics Using a Petal Nozzle", Journal of Propulsion and Power, Vol. 10, No. 5, Sept-Oct 1994, pp. 742-744.

6. Strykowski, P.J., Krothapalli, A. and Wishart, D., "Enhancement of Mixing in High-Speed Jets Using a Counterflowing Nozzle", AIAA Journal, Vol. 31, No. 11, November 1993, pp. 2033-2038.

7. Yu, K.H., Schadow, K.C., Kraeutle, K.J. and Gutmark, E.J., "Supersonic Flow Mixing and Combustion Using Ramp Nozzle", Journal of Propulsion and Power, Vol. 11, No. 6, Nov.-Dec. 1995.

8. Wishart, D., Krothapalli, A. and Mungal, M.G., "Supersonic Jet Control via Point Disturbances Inside the Nozzle", AIAA Journal, Vol. 31, No. 7, July 1993, pp. 1340-1341.

9. Ahuja, K.K. and Brown, W.H., "Shear Flow Control by Mechanical Tabs", AIAA Paper 89-0994, March 1989.

10. Samimy, M., Zaman, K.B.M.Q. and Reeder, M.F., "Effects of Tabs on the Flow and Noise Field of an Asymmetric Jet", AIAA Journal, Vol. 31, No. 4, April 1993, pp. 609-619.

11. Yu, K.H. and Schadow, K.C., "Cavity-Actuated Supersonic Mixing and Combustion Control", Combustion and Flame, 99, 1994, pp. 295-301.

12. Yu, K.H., and Schadow, K.C., "Control of Large-Scale Structures in Reacting Supersonic Jets", 8th ONR Propulsion Meeting, Oct. 1995.

13. Gutmark, E.J., Schadow, K.C., and Yu, K.H., "Mixing Enhancement in Supersonic Free Shear Flows", Annual Review Fluid Mechanics, 27, 1995, pp.375-417.

14. Kennedy, I.M. and Kollmann, W., "Role of Turbulent Shear Stress in Particle Dispersion", AIAA Journal, Vol. 31, No. 10, October 1993, pp. 1959-1960.

15. Longmire, E.K. and Eaton, J. K., "Active Open Loop Control of Particle Dispersion in Round Jets", AIAA Journal, Vol. 32, No. 3, March 1994, pp. 555-563.

16. Glawe, D.D. and Samimy, M., "Dispersion of Solid Particles in Compressible Mixing Layers", Journal of Propulsion and Power, Vol. 9, No. 1, Jan.-Feb. 1993, pp. 83-89.

17. Manser, J.R., "Solid Rocket Motor Plume Particle Size Measurements Using Multiple Optical Techniques in a Probe", M.S. Thesis, Naval Postgraduate School, March 1995

INITIAL DISTRIBUTION LIST

1. Defense Technical Information Center 2
   8725 John J. Kingman Rd., STE 0944
   Ft. Belvoir, VA 22060-6218
2. Dudley Knox Library 2
   Code 13
   Naval Postgraduate School
   Monterey, CA 93943-5101
3. Chairman 1
   Department of Aeronautics and Astronautics
   Code AA
   Naval Postgraduate School
   699 Dyer Road - Room 137
   Monterey, CA 93943-5106
4. Professor D. W. Netzer 3
   Department of Aeronautics and Astronautics
   Code AA/Nt
   Naval Postgraduate School
   699 Dyer Road - Room 137
   Monterey, CA 93943-5106
5. Professor O. Biblarz 1
   Department of Aeronautics and Astronautics
   Code AA/Bi
   Naval Postgraduate School
   699 Dyer Road - Room 137
   Monterey, CA 93943-5106

6. Curricular Officer, Code 37.....1
   Naval Postgraduate School
   Monterey, CA 93943-5000
7. Lt. Siwon R. Lee 2
   Weapons Test Squadron
   Naval Air Warfare Center, Weapons Division
   Naval Air Weapons Station Point Mugu, CA 93042